Complexity surrounding an apparently simple Fermi resonance in *p*-fluorotoluene revealed using two-dimensional laser-induced fluorescence (2D-LIF) spectroscopy

David J. Kemp, Laura E. Whalley, Adrian M. Gardner,[a] William D. Tuttle, Lewis G. Warner and Timothy G. Wright[b]

School of Chemistry, University of Nottingham, University Park, Nottingham NG7 2RD, UK

[a] Present Address: Stephenson Institute for Renewable Energy, University of Liverpool, L69 7ZF, UK

[b] Tim.Wright@nottingham.ac.uk

Abstract

Two-dimensional laser-induced fluorescence (2D-LIF) spectroscopy is a powerful tool allowing overlapped features in an electronic spectrum to be separated, and interactions between vibrations and torsions to be identified. Here the technique is employed to assign the 790–825 cm^{-1} region above the origin of the $S_1 \leftarrow S_0$ transition in *para*-fluorotoluene (*p*FT), which provides insight into the unusual time-resolved results of Davies and Reid [Phys. Rev. Lett. **109**, 193004 (2012)]. The region is dominated by a pair of bands that arise from a Fermi resonance; however, the assignment is complicated by contributions from a number of overtones and combinations, including vibration-torsion ("vibtor") levels. The activity in the 2D-LIF spectra is compared to recently reported zero-electron-kinetic-energy (ZEKE) spectra [Tuttle et al. J. Chem. Phys. **146**, 244310 (2017)] to arrive at a consistent picture of the energy levels in this region of the spectrum.

I. INTRODUCTION

Understanding the internal energy level structure in molecules is a key quest of chemical and molecular physicists. In particular, vibrations underpin our knowledge of the motion of the nuclei, which drives the making and breaking of bonds in chemistry. Chemistry can be further affected by the rotation of the molecule and the torsional motion of hindered rotor groups. All of these motions can couple, although this coupling can usually be treated as a perturbation on the overall vibrational energy structure. Building on work by Parmenter and coworkers,[1,2,3,4] recent work by the Lawrance group and ourselves has identified that vibration-torsional ("vibtor") coupling is of key importance in molecules that contain methyl groups: toluene, [5,6,7,8,9,10,11,] *para*-fluorotoluene (*p*FT) [12,13,14,15,16,17] and *para*-xylene (*p*Xyl).[17,18,19] Both a combination of an increasing density of states (DOS) and symmetry-allowed vibtor coupling have been invoked to rationalize the rapid increase in interactions that occur in such molecules,[17] which drives energy dispersal through a molecule.

In previous work, we have studied the lower-wavenumber regions of the $S_1 \leftarrow S_0$ transition in *para*-fluorotoluene (*p*FT) using resonance-enhanced multiphoton ionization (REMPI) and zero-kinetic-energy (ZEKE) spectroscopy;[12,13,17,20] while both we[13,20] and the Lawrance group[16] have also employed the technique of two-dimensional laser-induced fluorescence (2D-LIF).[21] The low-wavenumber region has been shown to be rich in interactions, involving torsional, vibrational and vibrational-torsional levels. (Since we work under jet-cooled conditions, and since we only partially resolve rotational structure, we do not directly consider interactions involving rotations.)

Earlier work on the $S_1 \leftarrow S_0$ transition in *p*FT has been reported by Cave and Thompson[22], Cvitaš and Hollas[23], Seliskar et al.[24] and Okuyama et al.[25] The latter two studies presented laser-induced fluorescence (LIF) spectra under jet-cooled conditions, giving assignments of some of the vibrational bands. Some of the low-wavenumber bands have been reassigned to vibration-torsion (vibtor) levels by Zhao,[3] and confirmed in recent work by our group[15] and that of Lawrance et al.[16] In an earlier paper from our group,[14] we had used the assignments of Okuyama et al.[25] in assigning ZEKE spectra recorded via various levels, unaware that some of the assignments of the lower-wavenumber features had been superseded by those in Zhao's thesis[3] – some of those latter reassignments are implicit in Ref. 2. In our earlier work,[14] we assigned the two levels at ~ 800 cm^{-1} to different totally-symmetric fundamentals on the basis of Okuyama et al's work,[25] but one of these was reassigned to an overtone level in Ref. 26. In Ref. 27, time-resolve photoelectron spectroscopy (tr-PES) was employed, and these same two features were assigned as a Fermi resonance (FR), involving the same levels noted in Ref. 26, although it was suggested that at least one other state might be interacting.

II. EXPERIMENTAL

The 2D-LIF apparatus has been described recently.[13] The vapour above room temperature *para*-fluorotoluene (99% purity, Alfa Aesar) was seeded in ~5 bar of Ar and the gaseous mixture passed through a General Valve pulsed nozzle (750 μm, 10 Hz, opening time of 180–210 μs) to create a free jet expansion. This was intersected at X/D ~20 by the frequency-doubled output of a single dye laser, operating with C540A. The fluorescence was collected, collimated and focused onto the entrance slits of a 1.5 m Czerny Turner spectrometer (Sciencetech 9150) operating in single-pass mode, dispersed by a 3600 groove/mm grating, and ~300 cm^{-1} windows of the dispersed fluorescence collected by a CCD camera (Andor iStar DH334T). At a fixed grating angle of the spectrometer, the excitation laser was scanned, and at each excitation wavenumber the image was accumulated for 2000 laser shots. This produced a 3D surface of fluorescence intensity versus the excitation laser wavenumber and the wavenumber of the emitted and dispersed fluorescence, termed a 2D-LIF spectrum.[21]

We have also recorded separate dispersed fluorescence (DF) spectra with higher averaging to get better signal to noise than simply taking a vertical slice through the 2D-LIF image. These DF spectra were recorded with the same spectrometer as for the 2D-LIF spectra, and were recorded three times accumulating over 5000 shots each time, and an average taken of these.

III. RESULTS AND ASSIGNMENTS

A. Nomenclature and labelling

1. Vibrational and Torsional Labelling

Since neither Wilson[28]/Varsányi[29] nor Mulliken[30]/Herzberg[31] notations are appropriate for the vibrations of *p*FT,[32,33] we shall employ the D_i labels from Ref. 33. (In other papers, we have included the labels used in previous work to aid the reader in referring to the different studies.[12,20]) Since the G_{12} molecular symmetry group (MSG) is appropriate for vibtor levels, we shall use these symmetry labels throughout. In addition, torsional levels will be labelled via their m quantum number. (The reader may find it useful to refer to previous work[9,10,11,15,18] if they are not familiar with these labels.) The correspondence between the C_{2v} point group labels and the G_{12} MSG ones are given in Table I. To calculate the overall symmetry of a vibtor level, it is necessary to use the corresponding G_{12} label for the vibration, and then find the direct product with the symmetry of the torsion (Table I), noting that a D_{3h} point group direct product table can be used, since the G_{12} MSG and the D_{3h} point group are isomorphic.

Under the free-jet expansion conditions employed here, the molecules are all expected to be cooled to their zero-point vibrational level and thus all $S_1 \leftarrow S_0$ pure vibrational excitations are expected to be from this level. In contrast, owing to nuclear-spin and rotational symmetry, the molecules can be in one of the $m = 0$ or $m = 1$ torsional levels.[18, 34]

2. Coupling and transitions

If an anharmonic fundamental is close in wavenumber to one or more combination or overtone vibrational levels that has the same overall symmetry, then "off-diagonal" anharmonic interactions can occur. The non-interacting levels are termed zero-order states (ZOSs), and their interaction leads to the formation of eigenstates that are linear combinations of these, and will be at different wavenumbers to the original ZOSs.[31] The simplest example of two interacting states is the classic Fermi resonance,[35] while for more than two levels we term this a complex Fermi resonance. For molecules that contain a hindered internal rotor, then the ZOSs can also be torsional or, if vibration-torsional coupling occurs, "vibtor" levels. The end result of such interactions is the formation of eigenstates which facilitate delocalization of energy through widespread motion of the molecule. Such couplings are only expected to be significant for small changes, $\Delta v \leq 3$, of the vibrational quantum number, and also for changes, Δm, of 0, ±3 or ±6 in the torsional quantum number in descending order of likely strength.[10,15,18,36,37]

In electronic spectroscopy, if we assume a non-coupled picture initially, then a zero-order vibrational, torsional or vibtor level can be bright (i.e. it has a significant transition intensity) or dark (i.e. it has no, or a very small transition intensity); these are often termed a zero-order bright (ZOB) state and a zero-order dark (ZOD) state, respectively. Following interaction, the resulting eigenstates will be composed of mixtures of ZOB and ZOD state character and so more transitions will become observable in the spectrum as a result of the interaction.

When designating excitations, we shall generally omit the lower level, since it will be obvious from the jet-cooled conditions; similarly, for emissions, we shall omit the upper level, as that will be obvious from the excitation and context. In the usual way, vibrational transitions will be indicated by the cardinal number, i, of the D_i vibration, followed by the number of quanta; torsional transitions will be indicated by m followed by its value. Finally, vibtor transitions will be indicated by a combination of the vibrational and torsional transition labels. If no m values are specified, then the transition refers to $m = 0$ and $m = 1$ levels, whose transition wavenumbers are expected to be coincident at the present resolution. We give two examples: (i) When accessed via emission from the origin, $20_1 m_2$ represents an excitation from the S_0 zero-point $m = 1$ level to the $m = 1$ level in the S_1 state, followed by emission to

the m = 2 level of the D_{20} level in S_0; and (ii) (29^2, 9_1) represents a dual excitation from the m = 0 and m = 1 levels of the S_0 zero-point level to both m levels of the S_1 state D_{29} overtone level, followed by dual emission to the corresponding m levels of the D_9 level in the S_0 state – note that these transitions will be coincident with our resolution.

The wavenumbers of the levels will be given with respect to the relevant zero-point level in each state, but noting that some excitations will originate from the m = 1 level in S_0 and those transition energies are given with respect to that level, as usual; the $S_1 \leftrightarrow S_0$ origin is located at 36860.0 cm^{-1} (Ref. 16). Very frequently, the most intense transition is expected to be that for which no change in the vibrational or both vibrational and torsional quantum numbers occurs; these will be designated $\Delta v = 0$ and $\Delta(v, m) = 0$ transitions. As has become common usage, we will generally refer to a level using the notation of a transition, with the level indicated by the specified quantum numbers, with superscripts indicating levels in the S_1 state and subscripts indicating levels in the S_0 state; since we will also occasionally be referring to levels in the ground state cation, D_0^+, we shall indicate those levels with a preceding superscripted + sign. Also, the eigenstates will usually be referred to by the dominant contribution from one of the ZOSs, with the context implying if an admixture of other ZOSs is present. 2D-LIF band positions can be indicated by a pair of (excitation, emission) wavenumbers, and corresponding transitions similarly.

B. Assignment of the spectra

1. Overall comments on the $S_1 \leftarrow S_0$ spectrum

In Figure 1, we show an overview of the excitation spectra across the region of interest recorded using both REMPI and fluorescence spectroscopies. To lower wavenumber it may be seen that there are two dominant features at 797 cm^{-1} and 804 cm^{-1}, with two other weaker features to higher wavenumber (one of which is not so clear in the integrated image, but features are evident in the 2D-LIF image in Figure 2). In Ref. 12 we discussed the assignment of this spectrum in detail, with the aid of ZEKE spectra and calculated vibrational wavenumbers, although some of the assignments were tentative. As noted above, the two intense bands have been assigned as arising from eigenstates that are dominated by one of 9^1 and 29^2 (Refs. 12, 26 and 27). Further, our ZEKE study[12] indicated a number of contributions to this region from overtones, combinations and vibtor levels, with many of these involving the three main levels (14^2, 29^1 and 11^1) that give rise to features seen in the spectrum at ~400 cm^{-1}, whose assignments were deduced from ZEKE[15,16] and, more recently, 2D-LIF spectra.[20] As well as 29^2, the other overtones and combinations of these three levels, and also transitions involving combinations with the vibtor level $14^1m^{6(-)}$, and possibly others, are expected. In the ZEKE study[12] it was also concluded that, as well as 9^1, the 12^114^1 and $12^1m^{6(-)}$ $S_1 \leftarrow S_0$ transitions contribute to this spectral region. Clearly 2D-LIF

spectroscopy will provide further evidence for or against these assignments and, as will be seen, give further insight into the activity and coupling.

In Figure 2 we present an overview of the recorded 2D-LIF spectrum across the 790–825 cm^{-1} excitation region. Vertical integration of the whole of this window of the spectrum gives a standard "LIF" spectrum, which is shown in Figure 1 where it is compared to the REMPI spectrum; it may be seen that both traces are very similar, indicating that the activity in this window of the 2D-LIF spectrum is a good representation of the overall activity of the transition. The 2D-LIF spectrum also shows a wealth of structure in the 0–300 cm^{-1} region, which is shown in Figure 3. In Figure 2, it will be noticed that there are two main vertical stripes of activity, corresponding to excitation via each of the two most intense bands in Figure 1 – this is in line with emissions arising from eigenstates that are composed of the same ZOSs. However, there are also cases where there is a pronounced difference in activity following excitation of one band and not the other, and such features are expected not to be associated with the two main eigenstates, but to arise from separate overlapping transitions. In addition, there is a third main stripe of emission activity to higher excitation wavenumber, with some common activity across the three main excitation features, with some weaker bands in between. Since we already have the assignments from our earlier ZEKE study,[12] we ought largely be able to assign the 2D-LIF spectrum by reference to the known S_0 and S_1 vibrational wavenumbers,[16,20,33] together with a knowledge of the positions of the torsional and low-wavenumber vibtor levels in the different states.[15,16]

Although we can obtain a conventional DF spectrum at a particular excitation wavenumber by taking a vertical cut through the 2D-LIF spectrum, we have often recorded such DF spectra separately, covering a wider range of emission wavelengths with an increased number of shots. In Figures 4–8 we show expanded sections of the 2D-LIF spectra, together with corresponding sections of the DF spectra, recorded via the centre of each of the 797 cm^{-1} and 804 cm^{-1} bands. Much of the activity is very similar from both of the bands, again confirming that these mainly arise from eigenstates that are largely made up from the same ZOSs.

2. Assignment of the main spectral activity

In our earlier ZEKE study,[12] a selection of spectra were recorded at excitation positions across the observed REMPI bands that are shown in Figure 1. From the changing activity, the make-up of the S_1 levels was deduced. However, the activity was not always as expected and the present 2D-LIF spectra should be able to shed some light on this. If we assume that we can just sum the band positions of the levels seen at 400 cm^{-1}, then we can predict the excitation wavenumber at which we expect to see the relevant combination and overtone 2D-LIF bands. It is likely, however, as the ZEKE study confirmed,

that levels are interacting with each other and also with the bright fundamental, 9^1, that appears in this spectral region; as such, the excitations could appear at shifted positions. We will now briefly discuss both the positions of the observed 2D-LIF bands, and their activity.

Previous ZEKE,[12] fluorescence[26] and tr-PES[27] studies agree that the two main excitation bands at 797 cm^{-1} and 804 cm^{-1} (Figure 1) correspond to eigenstates that largely correspond to contributions from 9^1 and 29^2, and this is confirmed by the present DF and 2D-LIF spectra in Figure 5. At first sight, the $\Delta v = 0$ region shown at the top of Figure 5 is perplexing, as it indicates large contributions from 29^2 to both levels, with the spectra being consistent with those of Zhao and Parmenter.[26] Similar behaviour was seen in the ZEKE spectra,[12] but an explanation was found in that the Franck-Condon factors (FCFs) when exciting via 9^1 were non-diagonal. Thus, it was observed that the $^+9^2$ ZEKE band was the most intense when exciting via the 797 cm^{-1} eigenstate, supporting the fact that it was dominated by 9^1, while the 804 cm^{-1} eigenstate is dominated by 29^2. Similar behaviour is seen here – see next paragraph. Also, there are contributions from other ZOSs to the spectrum, some of which may contribute to form the main eigenstates – see later in this subsection. Additionally, the ZEKE study[12] concluded that there were two overlapping features at 818 cm^{-1}: 11^2 and 12^114^1, but that these are not obviously in FR – these will be discussed later. Many of the other strong features in the 2D-LIF spectrum in Figure 2 may be deduced to arise from FC activity of the four main eigenstates dominated by each of 9^1, 29^2, 11^2 and 12^114^1, with particularly rich structure apparent at both of the 797 cm^{-1} and 804 cm^{-1} excitation regions. Indeed, occasionally the strong FC activity for certain features can obfuscate the assignment of the $\Delta v = 0$ band; however, considering the activity across the spectrum enables this to be achieved.

We first look at the $\Delta v = 0$ region of the 2D-LIF spectrum, at the top of Figure 5, together with the relevant sections of the DF spectra. The three pairs of bands here may be seen to correspond to three main emissions from each of the excitations, which may be assigned[16] to 14_2 (823 cm^{-1}), 9_1 (843 cm^{-1}) and 29_2 (850 cm^{-1}). Furthermore, it is also pertinent to observe that in the S_0 state, the two eigenstates made up from 9_1 and 29_2 are at 843 cm^{-1} and 850 cm^{-1}, while in the D_0^+ state, the two eigenstates are at 824 cm^{-1} and 832 cm^{-1}.[12] These levels are all close enough to be expected to be in Fermi resonance in each of the three electronic states, potentially complicating conclusions from DF or ZEKE spectroscopy regarding the make-up of the S_1 eigenstates. This means that, in any of the electronic states, the given labels merely reflect the dominant contribution of a ZOS to the eigenstate. However, we have found that emissions from totally-symmetric fundamentals, such as 11^1 (see Ref. 20), and levels in other unpublished work, give a higher intensity for the 9_1 band than the 9_2 and 14_2 bands. From such spectra, we can conclude that the 843 cm^{-1} S_0 eigenstate is made up of predominantly 9_1 character, but with some contribution from 29_2, and that the 850 cm^{-1} S_0 eigenstate is dominated by 29_2, with some contribution from 9_1. It is difficult to be sure of the mixings with the 14_2 state, for which the emissions could also simply be arising from FC activity from the totally-symmetric fundamentals.

The immediate observation from Figure 5 is that the activity of the main emission bands is very similar, with the 850 cm^{-1} emission band dominating from both the 797 cm^{-1} and 804 cm^{-1} levels. If the ZOSs were not interacting in the S_0 state, and if the FC intensity is dominant in the $\Delta v = 0$ region, then we would expect the emissions to the two S_0 levels to switch intensity from the two S_1 eigenstates, in contrast to the observations in Figure 5. As can be seen from Figure 7, however, the (9^1, 9_2) emission is much stronger than (29^2, 9_2), and hence the $\Delta v = 0$ intensities in Figure 5 are somewhat misleading. Overall, we concur with the previous conclusions from our ZEKE work[12] and the tr-PES study[27] that the main S_1 state eigenstates are each dominated by 9^1 and 29^2 to a similar extent, but that, as implied above, there is also the possibility of further interactions involving other ZOSs expected to be in this wavenumber region – see below.

A number of 2D-LIF bands appear with intensities that suggest they do not simply arise from FC activity. For example, we see significant non-totally-symmetric 29_1 and 28_1 bands (Figure 4) when exciting at 797 cm^{-1}, with the (totally-symmetric) 28_129_1 band being seen in Figure 5 – this is similar to behaviour seen when exciting via the origin (see Ref. 20). As we noted in Ref. 20, some caution is merited with the intensity of the 28_1 band, as this is at the expected wavenumber of the totally-symmetric 18_120_1 level, which was concluded to be FC active via the origin, and likely also to be active via totally symmetric fundamentals; the 28_129_1 band may also therefore have a contribution from $18_120_129_1$. It is clear that the 29_1 band arises from Herzberg-Teller (HT) vibronic activity, and this would also apply to $18_120_129_1$. Since these bands are seen to be present, but much weaker, when exciting at 804 cm^{-1}, the HT activity appears to be associated with the smaller 9^1 contribution to the latter eigenstate.

We now highlight the 1636 cm^{-1} emission band (Figure 7), which appears strongly when exciting at 804 cm^{-1}, but is much weaker when exciting at 797 cm^{-1}. This is assigned to 14_4, and indicates that the $14^2/29^1$ overlap seen at ~400 cm^{-1} is analogously present at 804 cm^{-1}, now involving 14^4 and 29^2 ; these are shifted up in wavenumber from the expected excitation positions, and this is consistent with interactions with 9^1. We might, therefore, also expect to see one or more 2D-LIF features corresponding to 14_229_1, which is expected at 1248 cm^{-1}. We see 14_229_1 clearly at 1243 cm^{-1} when exciting via 29^1 (see Ref. 20), but unfortunately such features are likely to be obscured by the strong 5_1 band seen in this region of the present spectra (see Figure 6), precluding definitive deductions regarding 14_229_1 activity.

Other excitations being seen to contribute to the ~400 cm^{-1} region[20] were $14^1m^{6(-)}$ and $14^120^2m^x$ and so we might expect to see combinations of these with 14^2, 29^1 and 11^1. (Note that the assignment of the m level associated with 14^120^2 was unclear, but was thought to be 1 or 2 – see Ref. 20.) Considering this, $14_3m_{6(-)}$ would be expected at 1443 cm^{-1}, and can be assigned to a band seen at 1449 cm^{-1} when exciting via 804 cm^{-1} (see Figure 6) which appears more weakly at 797 cm^{-1}; $14_229_1m_{6(-)}$ is expected at 1043 cm^{-1}, and can be assigned to a weak feature seen at 1040 cm^{-1} when exciting via 804 cm^{-1} (see Figure

5). The $11_1 14_1 m_{6(-)}$ vibtor band is expected at 1072 cm^{-1} (which is at the same wavenumber as a weak feature seen[20] when exciting at 398 cm^{-1}). Although a clear emission band is seen at this wavenumber (Figure 5), it is unexpectedly only seen when exciting at 797 cm^{-1} – indeed, this band will be assigned to a different transition below.

We note that the 11_1 band is more intense via the 804 cm^{-1} eigenstate (Figure 4), and associate this with additional FC activity from the various other levels contributing to this feature, as well as that from the 9^1 ZOS contribution.

There are three other ZOSs expected to contribute to this spectral region: 11^2, $11^1 14^2$ and $11^1 29^1$. We see a clear (11^2, 11_2) band at (818, 906) cm^{-1} (Figure 8) which is slightly shifted up from the expected excitation position of ~816 cm^{-1}. Exciting at 818 cm^{-1}, it is also possible to see extremely weak 11_1 activity on expanded views of Figure 8, but more sizeable 11_3 activity is evident. There is some 11_2 activity when exciting at 797 cm^{-1}, with very faint activity at 804 cm^{-1}, which is consistent with FC activity.

Weak $11_1 29_1$ emission is seen at 877 cm^{-1}, as expected (see Figure 8), and has two islands of activity: one at 809 cm^{-1}, and one at 797 cm^{-1}. The latter is likely related to the 29_1 HT activity at that wavenumber, suggesting the former is the $\Delta v = 0$ band, and this is close to the expected position. Note that the $11^1 29^1$ level is of a_1'' symmetry, and so unable to couple to the 9^1 band anharmonically, explaining its weakness; there are, however, possibilities of other vibtor levels with which it could interact and this, together with intrinsic anharmonicity in forming the combination band, could explain the slightly shifted position.

The $11_1 14_2$ band is expected at ~1277 cm^{-1}, and clear features are seen at 1276 cm^{-1} (see Figures 6 and 8). There are four islands of activity, at 797, 804, 811 and 818 cm^{-1}, with the first two being far stronger than the latter two. We note that the latter may contain some contribution from 29_3, which can be seen when exciting via 29^1 (Ref. 20), but this is expected to be significantly weaker for the present excitation, owing to symmetry. The ZEKE spectra[12] show $^+11^1 14^2$ activity at 804 and 818 cm^{-1}, but not obviously so at 797 cm^{-1}. One complicating factor is FC activity from the two main 797 cm^{-1} and 804 cm^{-1} eigenstates, and it can be seen that there are clear 14_2 bands at these excitation positions (Figure 5), and so it is not unexpected to see $11_1 14_2$ bands also; hence, these are assigned to FC activity, together with the (818, 1276) cm^{-1} band. These arguments are also supported by the clear FC activity from 18_2 at the two lower wavenumber positions (see Figure 5); this emission is also seen weakly when exciting at 818 cm^{-1} – see Figure 8). From this, we conclude that the $11_1 14_2$ band is demonstrating FC activity from 9^1, 29^2 and $12^1 14^1/11^2$. We thus conclude that the band at (811, 1276) cm^{-1} is likely to be the $\Delta v = 0$ band.

The reasons noted above for the very weak $11_1 29_1$ band also apply to $14_2 29_1$ and explain why it is not obviously seen in our spectra, although, as noted, it could be overlapped with the strong 5_1 band. These reasons do, however, makes it surprising that the $14_1 29_1 m_{6(-)}$ band is seen at 1042 cm^{-1}, suggesting that this could arise by other coupling mechanisms, perhaps involving 29^2.

We now discuss the $12_1 14_1$ activity – see Figure 8. This appears at three positions with the $\Delta v = 0$ band clearly seen at 818 cm^{-1}, and the other islands of emission activity being via excitations at 797 and 804 cm^{-1}. It is seems likely these last two features must arise from FC activity from the two main eigenstates, as it is difficult to see that 9^1 and 29^2 are interacting so strongly with $12^1 14^1$ that the resulting eigenstates end up so far apart; moreover, we do not see any evidence of 9_1 nor 29_2 activity when exciting via $12^1 14^1$ – see Figure 8. Interestingly, the same islands of activity for $12_1 14_1$ occur with the much weaker 11_3, although the activity at 804 cm^{-1} seems stronger than that at 797 cm^{-1}, which is the opposite of the $12_1 14_1$ activity. The 11_3 activity can be contrasted with that of 11_2, which is actually stronger when exciting at 797 cm^{-1} than 804 cm^{-1}. We also remark that there is a curious coincidence here, whereby in the S_1 state the 11^2 and $12^1 14^1$ levels are almost isoenergetic, while in the S_0 state the 11_3 and $12_1 14_1$ levels almost coincide; it is also the case that the latter corresponding cation levels are similarly very close in energy.[12] There is not, however, any unambiguous evidence of interactions between the noted levels in any of the three electronic states.

The relatively strong 1518 cm^{-1} emission band (Figure 6) when exciting at 804 cm^{-1} can be assigned as $14_3 20_2 m_x$, and would be the counterpart of the $14_1 20_2 m_x$ band (702 cm^{-1}) seen when exciting at ~400 cm^{-1};[20] this would be consistent with the clear 702 cm^{-1} emission seen at this excitation position (Figure 4). (Recall from above that in Ref. 20 we could not definitively decide on the associated *m* level.)

In the above, we have seen that most of the bands we observed[20] when exciting at ~398 cm^{-1} also appear in this region, each in combination with 14_2 and 29_1, but with their $\Delta(v, m)$ bands at 804 cm^{-1}. This is particularly surprising, since the expected band positions might suggest that these would appear close to 797 cm^{-1}. This appears to be the result of a remarkable coincidence caused by the movement of the various levels via their interaction with 9^1, and possibly in tandem with the positive anharmonicity of the 14^n progression, seen for *p*DFB.[38,39] It is also evident that there is greater 14_2 activity when exciting at 804 cm^{-1} than there is at 797 cm^{-1} (see Figure 5), which would be consistent with these other S_1 levels arising from 14^2 combinations lying at this wavenumber.

Above, we have noted that the 1071 cm^{-1} emission band (Figure 5) is at the expected position for $11_1 14_1 m_{6(-)}$, but that it is unexpected that this would be almost exclusively localized at 797 cm^{-1}, particularly given the spread of activity of $11_1 14_2$ across the spectrum (and noting that the 14^2 and $14^1 m^{6(-)}$ levels are almost isoenergetic and interacting[12,16,20]). Since we would expect $11^1 14^1 m^{6(-)}$ to appear at an excitation position of 806 cm^{-1}, it seems unlikely that any interaction would be enough to

cause it to lie very close to the 797 cm^{-1} eigenstate, and would not be consistent with the localized activity. Further, close inspection of the $14_1m_{6(-)}$ band profile (seen at 618 cm^{-1} in Refs 16 and 20) shows these to be somewhat different, and additionally the 1071 cm^{-1} band is found not to be enhanced when exciting via 11^1. Since the band appears relatively localized in excitation position, and being totally symmetric, this is likely to be the $\Delta v = 0$ band; hence, we sought another assignment of this band, with the most likely candidate being 15_120_1. This would suggest that the wavenumber of D_{15} in the S_1 state is 687 cm^{-1}, which is still in reasonable agreement with the calculated value, but would require our previous value[12] of 678 cm^{-1} to be revised. The latter came from a very tentative assignment of a $\Delta(v, m) = 0$ ZEKE band to $^+15^1m^{3(-)}$. If we then cross-check with the ZEKE spectrum, we would expect the $^+15^120^1$ level to lie at ~1109 cm^{-1} using the calculated value for D_{15} in the cation, which would excellently match the ZEKE band at 1112 cm^{-1} seen when exciting at these corresponding wavenumbers;[12] pleasingly, this also matches the extent of this feature to lower wavenumber where the 1112 cm^{-1} ZEKE band is prominent. That ZEKE feature was assigned to $^+14^229^1$ in Ref. 12, but as we have noted, we are unable to discern 14_229_1 emission in our 2D-LIF spectra, but it may be masked by the strong 5_1 features – we shall come back to this later. Since we expect $11^114^1m^{6(-)}$ to be interacting with 11^114^2, and since the $\Delta v = 0$ band of the latter is weak, then the $11_114_1m_{6(-)}$ band is also expected to be weak, and presumably this is the reason for its non-observation; further, if it were interacting, then we would expect to see activity at different excitation wavenumbers.

In our previous ZEKE study,[12] we also assigned a band at 1171 cm^{-1} to $^+12^1m^{6(-)}$, seen clearly when exciting at 794 cm^{-1} and at various positions across the 797 cm^{-1} band. The corresponding 2D-LIF band would be expected to have an emission of ~1161 cm^{-1}, but there is no such band seen when exciting at 797 cm^{-1}. (The only possible candidate is a feature at ~1174 cm^{-1}, which lies just above the 10_111_1 band, and appears to be wholly localized around 797 cm^{-1}, but this seem too distant in wavenumber to be likely; further, the S_1 excitation position for $12^1m^{6(-)}$ would be expected to be significantly higher than 797 cm^{-1} in the absence of any significant interactions.) There are a number of pure vibrational assignments for the 1174 cm^{-1} feature, with $14_119_129_1$ perhaps being the most likely on the grounds that it is totally symmetric (and so could be FC active), and contains 29_1 character (given the activity of 29_1 at this excitation position). Although, we find little enhancement of this feature when exciting via 29^1, this may be because of the difference in symmetry. Alternatives such as a HT-active a_1'' symmetry level, e.g. $14_120_130_2$, would not be expected to be so intense. Either way, the reassignment of the ZEKE band meets the expectation that the $12^1m^{6(-)}$ state would not be expected to lie so far from 12^114^1, since the 14^1 and $m^{6(-)}$, and 14^2 and $14^1m^{6(-)}$, pairs of levels are each close together in the S_1 state,[12,16] and so it is difficult to see what could displace the $12^1m^{6(-)}$ level so far away from 12^114^1. Further inspection of the spectra reveals a very weak 2D-LIF feature at (820, 1159) cm^{-1} that would be consistent with being the ($12^1m^{6(-)}$, $12_1m_{6(-)}$) band. We now, however, would need to reassign the 1171 cm^{-1} ZEKE band. One possibility is $^+7^1$ FC activity from totally symmetric levels such as 15^120^1 and 9^1. However, this

ZEKE band appears clearly across the 797 cm^{-1} and 804 cm^{-1} excitation regions and it is unclear why it would be so relatively intense when exciting at ~797 cm^{-1}. Another possibility is $^{+}9^{1}14^{1}$, which would tie in with the activity of $^{+}14^{1}$ commonly seen in ZEKE spectra of substituted benzenes, and discussed in our recent paper on *p*-difluorobenzene;[39] additionally, the $^{+}9^{1}14^{1}m^{1}$ level is possible as it is symmetry allowed from $m = 0$ levels of totally-symmetric vibrations.

We summarize the comparison of the present 2D-LIF and DF spectra with the ZEKE spectra of Ref. 12 as follows. First, the main 2D-LIF assignments are consistent, with the 797 cm^{-1} level giving non-diagonal FCFs for the 9_1 and 9_2 bands, and confirming the 797 cm^{-1} level is made up predominantly of 9^{1}; similarly, the ZEKE and 2D-LIF spectra are both strongly indicative of the 804 cm^{-1} band being dominated by 29^{2}. Also clear in both sets of spectra are the contributions from 11^{2} and $12^{1}14^{1}$ at 818 cm^{-1}, $11^{1}29^{1}$ at 807 cm^{-1}, and $11^{1}14^{2}$ at 811 cm^{-1}. We have noted the reassignment of the 1112 cm^{-1} ZEKE band, previously associated with $^{+}14^{2}29^{1}$, as now being indicative of $15^{1}20^{1}$ activity at 797 cm^{-1}; while the 1171 cm^{-1} ZEKE band, rather than indicating $12^{1}m^{6(-)}$ activity at 797 cm^{-1}, is merely reflecting FC activity of $^{+}7^{1}$ or $^{+}9^{1}14^{1}m^{1}$ The 14^{4} activity was difficult to pin down in the ZEKE study, but there was evidence for the $^{+}14^{4}$ ZEKE band appearing across the 804 cm^{-1} excitation region, and this seems to be confirmed in the 2D-LIF. It is difficult to pick out ZEKE bands arising from $^{+}14^{3}m^{6(-)}$, expected at 1237 cm^{-1}, $^{+}29^{1}14^{1}m^{6(-)}$ expected at 953 cm^{-1}, nor $^{+}11^{1}14^{1}m^{6(-)}$ expected at 977 cm^{-1}. The lack of $^{+}11^{1}14^{2}$ ZEKE bands in the 797 cm^{-1} excitation region are consistent with the S_1 level not interacting significantly with 9^{1}, but with other ZOSs that are contributing to the 804 cm^{-1} band.

Note that in our recent paper on the 400 cm^{-1} region,[20] we assigned a 489 cm^{-1} 2D-LIF emission band to $20_2m_{6(+)}$ arising from interaction with 14^{2}. We can see a weak feature at (805, 1308) cm^{-1}, which can be assigned to $14_220_2m_{6(+)}$ – expected at 1311 cm^{-1}. The $14^{2}20^{2}m^{6(+)}$ level would analogously be expected to interact with 14^{4}, but we noted in Ref. 20 that such an interaction is likely to be weak and be highly dependent on the levels being extremely close in energy; indeed, this feature does have a localized intensity.

3. Comments on other selected features

In Figure 4, we see a very weak feature at (797, 558) cm^{-1}, assigned to 14_120_1, that is barely visible when exciting at 804 cm^{-1}; this is consistent with a corresponding emission observed in Ref. 16. A weak band at 633 cm^{-1} seems to be the same band seen when exciting at 364 cm^{-1},[20] assigned to $14_120_1m_4$ and can be expected to be active from $14^{3}20^{2}m^{1}$. The band at 670 cm^{-1} is 19_2 consistent with an emission reported by Gascooke et al.[16]

An emission band at 731 cm^{-1} is seen clearly when exciting at 797 and 804 cm^{-1} (see Figure 4) and was also seen via the origin,[20] and it has been assigned to 10_1. A second very close emission feature is evident at 733 cm^{-1} when exciting via 797 cm^{-1}, which can be discerned in the DF spectra; the most likely assignment is 29_130_1, and ties in with the observed stronger $28_129_1/18_120_129_1$ band when exciting at 797 cm^{-1}. It is interesting to note that 29_130_1 is not enhanced when exciting via 29^1 (Ref. 20), which can be attributed to its different symmetry; this could thus be evidence for the enhancement of the $28_129_1/18_120_129_1$ band when exciting via 29^1,[20] as being due to a significant $18_120_129_1$ contribution.

There is a weak emission band at 863 cm^{-1} that is active across the three main regions of the spectrum. A possible assignment is 29_2m_2, accessed via a $\Delta m = 3$ transition, but this would be expected to be weak. Other possibilities are $14_120_3m_2$ or $11_114_1m_1$, and we favour the latter as there is a weak secondary feature at 870 cm^{-1}, which seems likely to be $11_119_1m_4$. Then these two bands are analogous to the $14_1m_1\ldots19_1m_4$ interaction seen by Gascooke et al.[16] and the $14_2m_1\ldots14_119_1m_4$ interaction seen in our recent work.[20]

A weak emission band at 895 cm^{-1} also appears at the three main excitation positions, and suggests assignments as $9_1m_{3(+)}$ or $11_129_1m_2$, with the latter favoured as the band is more intense when exciting at 797 cm^{-1}, as is the 29_1 band; also, since the level has e'' symmetry, it is symmetry-allowed at the three main positions from the $m = 1$ levels of the dominant ZOSs; the absence of 9_1 emission when exciting at 818 cm^{-1} makes the $9_1m_{3(+)}$ assignment unlikely. There are several weak bands around 900 cm^{-1}, and although one of these is clearly 11_2, as noted in the above, the assignments of the others are uncertain, with vibtor levels related to 9_1 and 29_2 being candidates for some of these.

In the 1200–1300 cm^{-1} emission region (see Figure 6) there are a series of bands that are straightforwardly assigned. The first three bands at 1210, 1223 and 1236 cm^{-1} have assignments of 6_1, 13_114_1 and 5_1. These assignments are consistent with bands observed via other levels and presented in Ref. 20; and the appearance of 13_114_1 is consistent with the observed activity of the 14_2 and 12_114_1 bands. To slightly higher wavenumber are the overlapped 11_114_2 and 29_3 bands, whose presence can be ascertained from the differing activity when exciting via different intermediate levels.[20] We find that the 11_114_2 band is more intense via 11^1 and 797 cm^{-1}, while the 29_3 band is more intense via 29^1,[20] but we expect the contributions from the latter to be minimal in this excitation region. At 1294 cm^{-1} is 9_111_1, and at 1301 cm^{-1} we see 11_129_2, with the latter being most intense when exciting via 797 cm^{-1} and 804 cm^{-1}, consistent with the $\Delta v = 0$ region. There are three other prominent features to higher wavenumber in this region: 1364 cm^{-1}, which is assigned to 12_114_1; 1394 cm^{-1}, which is assigned to 17_2; and 1487 cm^{-1}, which is assigned to 9_128_1, and can be seen to be more intense via 797 cm^{-1}. Lastly, there appears to be a double band with maxima at 1515 cm^{-1} and 1519 cm^{-1}; the latter has already been assigned to

$14_3 20_2 m_x$ (see above). Taking into consideration the expected activity of various combination bands via different intermediates, our favoured assignment of the 1515 cm^{-1} band is to $14_1 16_1 30_1$, but this is tentative.

The 1600–1750 cm^{-1} emission region (see Figure 7) is not initially straightforward to assign as there are multiple overlapping bands, with possible interactions between the contributing S_0 levels. DF spectra recorded from different intermediate levels (see Figures 7 and 9) are, however, very useful. This region is complicated since it is expected to show overtones and combination bands of the levels that contribute to the $\Delta v = 0$ (~800 cm^{-1}) region; it is also where 11_1 and 29_1 combinations with the S_0 levels seen at 1200–1300 cm^{-1} are expected to appear; and there is also the possibility of new fundamentals and other combinations and overtones. Furthermore, there is the likelihood of overlapping features and interactions between levels. In Figure 9 we show spectra recorded via six different intermediate levels: 0^0, 14^2, 29^1, 11^1 and the 797 cm^{-1} and 804 cm^{-1} levels. The 11_1 combinations with the 1200–1300 cm^{-1} features are easy to pick out: $6_1 11_1$, $11_1 13_1 14_1$ and $5_1 11_1$, as are the corresponding combinations with 29_1. The strong 9_2 band is also easy to identify, and shows clearly that the (9^1, 9_2) band is significantly more intense than (9^1, $9_1 29_2$) and (9^1, 29_4), confirming that the 9^1 contribution to the 797 cm^{-1} eigenstate is dominant. (Note that the $9_1 29_2$ and $5_1 11_1$ bands are very close in wavenumber and partially overlapped, but have very different activities via different intermediate levels.) Interestingly, although the (29^2, $9_1 29_2$) band is more intense than the (9^1, 9_2) and (9^1, $9_1 29_2$) bands, we see that the (9^1, 29_4) band is more intense than (29^2, 29_4) – see Figure 7. Also clear are the $9_1 14_2$ and $14_2 29_2$ bands at 1664 and 1668 cm^{-1}. It can be seen that the $6_1 29_1$, $13_1 14_1 29_1$ and $5_1 29_1$ bands are all enhanced via 797 cm^{-1} compared to 804 cm^{-1}, consistent with the HT activity of 29_1 when exciting at 797 cm^{-1}.

IV. DISCUSSION

In Figure 3, we show the 0–310 cm^{-1} region of the DF spectra obtained when exciting via the origin, and each of the 797 cm^{-1} and 804 cm^{-1} bands. The features have been assigned and discussed in depth in Ref. 16, to which the reader is referred. It may be seen that the structure is very similar in all three cases, and in particular that there are features that arise from both the $m = 0$ and $m = 1$ levels, with similar relative intensities in each case.

We have noted that in the picosecond tr-PES[27] study, the two S_1 eigenstates at 797 cm^{-1} and 804 cm^{-1} were concluded to arise from a Fermi resonance, as deduced from monitoring the time-dependent signal from ionization to the origin using photoelectron spectroscopy, and that is consistent with the deductions here and in Ref. 12. Of particular interest, however, is the observation that a large amount

of the intensity was lost rapidly (over 30 ps) when these two eigenstates were excited coherently – this was interpreted as rotational dephasing involving one of the torsional levels in each of the two vibrational eigenstates.

Those time-resolved experiments made use of picosecond lasers, whose linewidth is ~ 15 cm^{-1}. As such, more than one eigenstate is excited coherently, forming a wavepacket – i.e. a coherent superposition of more than one eigenstate. As with the nanosecond experiments, projection of the excited state eigenstates (in that case, a wavepacket) onto those of another state (in that case, the cation) can, in principle, allow the ZOS make-up to be ascertained, particularly if the corresponding ZOSs are well-separated in the cation. (It should be noted that in the picosecond experiments, the populations of the eigenstates do not change with time, unless there is some additional photophysical process occurring: the variations one sees in the time-resolved photoelectron spectra are caused by the moving in and out of phase of the eigenstates in the wavepacket.) If such variations can be recorded over a large enough timescale, then Fourier transformation can be used to obtain the energy separations between the component eigenstates,[27] and these should, of course, be consistent with the separation of corresponding bands seen in a REMPI or LIF experiment. Such a Fourier transform was performed in that work,[27] and two peaks were seen, one at 6.7 cm^{-1} and one at 6.2 cm^{-1}, with the former being the more intense and sharp, while the latter was much weaker with a broader structure. The 6.7 cm^{-1} separation matches that between the 797 cm^{-1} and 804 cm^{-1} excitation bands in Figure 1. The 6.7 cm^{-1} separation was hypothesised as arising from a particular m level of the two vibrations, with the 6.2 cm^{-1} separation arising from the other populated m level in the same levels (recalling that both $m = 0$ and $m = 1$ levels will be populated). The separation was suggested as being caused by the $m = 0$ and $m = 1$ levels having slightly different rotational constants. It was then suggested that the rapid loss of intensity within the first 30 ps arose from rotational dephasing, which was suggested as arising from a rotational-level dependent coupling term – it was noted that such a coupling could not be simply anharmonic, since this would not have a rotational dependence. The rotational dephasing would occur as a result of destructive interference between the many coherently excited rotational levels corresponding to the same m level in the two different vibrational eigenstates, caused by an m-specific (and J, K-dependent) interaction. Since this effect is expected to be very small, it would be consistent with the small difference in the two spacings of the eigenstates reported in Ref. 27. Further, this would explain why, in Figure 3, we see the whole set of torsional levels via both the 797 cm^{-1} and 804 cm^{-1} levels at what appear to be identical emission wavenumbers – the dephasing *only* occurs as a result of the two eigenstates being coherently excited. At the resolution in our spectra, we are unable to see any obvious difference in spacings of the various torsional levels in Figure 1, nor in the separation of the various $\Delta(v, m) = 0$ bands. As noted in Ref. 27, what is required is for there to be one or more interactions with nearby ZOSs that is m specific,

and which causes a sufficient perturbation to lead to a *J, K*-dependent perturbation to the rotational energy levels, which we now explore.

In the above, we have noted several levels that are coincident with one or more of the main two eigenstates at 797 cm^{-1} and 804 cm^{-1}; however, we also require the levels to be interacting for the *m*-specific interaction to occur. Hence, for example, the $15^{1}20^{1}$ level could not be a cause of the perturbation in rotational constants as it is not interacting to any noticeable extent, and there would be no reason why the interaction would not take place in both *m* levels. The latter comment also applies to levels such as $11^{1}14^{2}$, 14^{4}, 11^{2} $12^{1}14^{1}$ etc. However, the $14^{3}m^{6(-)}$ or $14^{3}20^{2}m^{x}$ levels would each be expected to interact only with one of the *m* levels and so could cause the required perturbation. This seems most likely to happen for the 804 cm^{-1} eigenstate(s), where the activity from these levels is localized. One possibility would be the interaction between 14^{4} and $14^{3}m^{6(-)}$, which is analogous to the $14^{1}\ldots m^{6(-)}$ and $14^{2}\ldots14^{1}m^{6(-)}$ interactions discussed in Refs. 12, 16 and 20; in particular, this interaction has been noted in Ref. 16 as being sensitive to the rotational levels moving in and out of resonance, and so perturbing the rotational structure. Thus, the interactions between $14^{4}m^{0}$, $14^{3}m^{6(-)}$ and $9^{1}m^{0}$ may well have a rotational dependence and cause $m = 0$ rotational levels to have slightly different wavenumber separations than the corresponding $m = 1$ ones. We also observe that it is possible that some of the complications discussed in the analysis of the time-resolved data in Ref. 27 could be attributable to contributions from the various ZOSs to this region, which would also be excited in those experiments. It is clear, however, that the loss of intensity in the tr-PES study cannot be incipient dissipative intramolecular vibrational redistribution (IVR), as then we would expect a significant, broad underlying background in the present nanosecond excitation spectra, but this is not seen.

Coming back to our recent work[20] on the bands at ~ 400 cm^{-1}, we there noted that there are a significant number of bands involving the low-wavenumber, out-of-plane modes, D_{14} and D_{20}, commensurate with these modes coupling to the torsional motion of the methyl group, and this is also the case in the higher wavenumber region focused on in the present work. These modes, and to some extent D_{19}, seem to be key in providing routes for the methyl group to couple to the vibrational motions. Because of symmetry constraints, the main routes are coupling with the $m = 3(-)$ level for D_{20} and D_{19} and the $m = 6(-)$ level for D_{14}. Coupling between in-plane vibrations also occurs – for example, D_{29} with $m = 3(+)$.

In Refs. 13 and 20, we also highlighted the role of the $m = 1$ levels in enhancing the coupling between levels, something that is implicit in the energy level diagrams of Ref. 16. These open up routes to coupling between vibtor levels arising from vibrations of different C_{2v} symmetry, which lead to a rapid rise in the possibilities for interactions, albeit somewhat sporadically at low energy.[17]

We have seen that there is strong evidence for the interaction between 9^1 and 29^2, both from the tr-PES study,[27] and also from the corresponding FC activity, but with differing intensities in both the ZEKE study[12] and the present 2D-LIF study. Furthermore, other activity in the ZEKE and 2D-LIF spectra indicate that there are contributions from other ZOSs, and that these have moved from their expected positions, providing evidence of interactions. We also see that for "clean" emission features, such as 1518 cm^{-1} and 1636 cm^{-1}, there is weak activity at 797 cm^{-1} as well as the very dominant activity at 804 cm^{-1}, and this confirms the interactions of some of the ZOSs with 9^1. In contrast, although we see clear $12_1 14_1$ activity when exciting at 797 cm^{-1} and 804 cm^{-1}, the lack of any partnering activity of 9_1 or 29_2 when exciting via $12^1 14^1$ suggests no interaction with those levels, and the former activity is FC in nature. Although a quantitative picture is not straightforward to extract, we believe the picture of the interactions is qualitatively as follows. The 29^2 ZOS lies above 9^1, and this is the main interaction. The 14^4 level also lies above 9^1, which may arise as part of the overall set of interactions, including $9^1 \ldots 29^2$, or because of positive anharmonicity in the 14^n progression; either way, the 14^4 and 9^1 levels also interact. The result is that 29^2-dominated and 14^4-dominated eigenstates are essentially at the same energy (804 cm^{-1}). Since 14^2 and $14^1 m^{6(-)}$ interact strongly[12,15,16] then this gives some rationale as to why the $14^3 m^{6(-)}$ level also appears at 804 cm^{-1} (since 14^2 and $14^1 m^{6(-)}$ are almost isoenergetic)[16,20] although there is no *a priori* reason to expect the interactions of different ZOSs with 14^4 and $14^3 m^{6(-)}$ to be the same. In contrast, the $11^1 14^2$ level appears at a lower wavenumber, implying that the interactions between 9^1 and this level are weaker; the appearance of $11^1 29^1$ to lower wavenumber is consistent with its different symmetry from 9^1. It is surprising that the $14^1 29^1 m^{6(-)}$ level also appears at 804 cm^{-1}, and this is likely the result of a number of interactions. We cannot be definitive about the positions of $11^1 14^1 m^{6(-)}$ and $14^2 29^1$, as unambiguous emission bands are not seen for these. We might expect $11^1 14^1 m^{6(-)}$ to be close to $11^1 14^2$ and $14^1 29^1 m^{6(-)}$ to be close to $14^2 29^1$, but as noted above, the interactions could be different for these ZOSs. We assigned an emission band at 1071 cm^{-1} to $15_1 20_1$, even though this was at the wavenumber expected for $11_1 14_1 m_{6(-)}$, and noted that the $15^1 20^1$ level does not appear to be interacting with 9^1 or 29^2. As commented above, via the 797 cm^{-1} and 804 cm^{-1} eigenstates we see $12_1 14_1$ FC emission, and we conclude the $12^1 14^1$ level is not interacting with 9^1. Moreover, even though 11^2 and $12^1 14^1$ are almost degenerate, they do not seem to be interacting in S_1, as their activity across the spectra is different; similar comments apply to $12_1 14_1$ and 11_3 in S_0. Finally, we have concluded that the $^+12^1 m^{6(-)}$ band was misassigned in our previous ZEKE study,[12] and we tentatively conclude that the corresponding S_1 level may be located close to $12^1 14^1$.

V. CONCLUSIONS

In this work, it has been seen that, although at first sight the REMPI/LIF excitation spectra appear to indicate a rather straightforward pairwise classic Fermi resonance interaction, in fact the picture is

significantly more complicated, in agreement with the conclusions of the ZEKE study[12] and, in part, consistent with the conclusions of the tr-PES study.[27] It is clear, however, that although there are a fair number of ZOSs contributing to the 790–825 cm^{-1} region, the present results and those of Ref. 27 indicate that we are still in the restricted IVR regime, but with the situation being far more complicated than a simple Fermi resonance. In previous work,[40] we have discussed the factors that affect experimental observations relating to IVR, and one of these was the temperature of the molecules. This, we believe, underlies the indications of wider-ranging IVR implicit in the DF spectra obtained via 9^1 and even via the ~400 cm^{-1} levels in a 300 K sample of *p*FT,[41] probably driven by thermally-populated torsional and rotational levels.

Lastly, as with the $14^2…14^1m^{6(-)}$ interaction which has localized rotation-level dependent coupling,[16] we find that several other bands appear to show unexpected intensity profiles (e.g. bands at 973 cm^{-1} and 993 cm^{-1}), and this may be evidence for similar effects.

In summary, we have shown that 2D-LIF is a powerful tool in revealing overlapping bands in an excitation spectrum and separating these to facilitate their assignments. The spectra also help to reveal interacting levels via the different intensities seen when exciting at different positions. In some cases, complications arise from separating FC activity from cross-activity arising from interacting ZOSs, but considering other activity can often clarify this. The technique is particularly useful in cases such as here, where a (not too large) number of ZOSs are interacting in complex Fermi resonances, and where the anharmonic shifts in levels cause levels to move, making it more difficult to identify them in a simple excitation spectrum. Further, the much more complete dataset represented by a 2D-LIF spectrum provides greater reliability regarding the interpretation of the activity; however, the “2D-ZEKE” spectra we have published[12] are complementary, as they project the S_1 levels onto a different electronic state, and so help to confirm assignments.

Acknowledgements

We are grateful to the EPSRC for funding (grant EP/L021366/1). The EPSRC and the University of Nottingham are thanked for studentships to D.J.K., W.D.T. and L.E.W. The Royal Society of Chemistry are thanked for an Undergraduate Summer Bursary for L.G.W. We are grateful for discussions with Warren Lawrance and Jason Gascooke (Flinders, Adelaide) and Katharine Reid (Nottingham).

Table I: Correspondence of the C_{2v} point group symmetry classes with those of the G_{12} molecular symmetry group. Also indicated are the symmetries of the D_i vibrations and the different pure torsional levels.[a]

C_{2v}	G_{12}	D_i [b]	m
a_1	a_1'	D_1–D_{11}	0, 6(+)
a_2	a_2'	D_{12}–D_{14}	6(-)
b_1	a_2''	D_{15}–D_{20}	3(-)
b_2	a_1''	D_{20}–D_{30}	3(+)
	e'		2,4
	e''		1,5

[a] Symmetries of vibtor levels can be obtained by combining the vibrational symmetry (in G_{12}) with those of the pure torsional level, using the D_{3h} point group direct product table.

[b] The D_i labels are described in Ref. 33, where the vibration mode diagrams can also be found.

Figure Captions

Figure List

1. Overview of the REMPI spectrum and integrated 2D-LIF spectrum over the range of interest – see text.

2. Overview of the 2D-LIF spectrum across the whole range of interest. The spectral intensities are represented by colours, with red being the most intense through to blue being the least; black represents the zero background.

3. Expanded view of the 2D-LIF spectrum of *p*FT in the 0–310 cm^{-1} region exciting via the 797 cm^{-1} and 804 cm^{-1} eigenstates. The spectral intensities are represented by colours, with red being the most intense through to blue being the least; black represents the zero background. We also show the corresponding DF spectra from these two levels and the origin. This region covers the main torsion and vibtor levels associated with the D_{20}, D_{19} and D_{30} vibrations. The appearance of the spectrum via the origin is very similar to that recently published by Gascooke et al. in Ref. 16, where it is discussed in detail. The relative intensities in the 2D-LIF spectrum are as recorded, while the DF spectra have been adjusted to be qualitatively in agreement with the 2D-LIF spectrum, but with some regard to presentational clarity. Thus, the relative intensities within the same DF trace will be reliable, but not necessarily when comparing between two traces.

4. Expanded views of the 2D-LIF and DF spectra for the 390–790 cm^{-1} region, exciting via the 797 cm^{-1} and 804 cm^{-1} eigenstates. The spectral intensities are represented by colours, with red being the most intense through to blue being the least; black represents the zero background. See text for discussion of the assignments. The relative intensities in the 2D-LIF spectrum are as recorded, while the DF spectra have been adjusted to be qualitatively in agreement with the 2D-LIF spectrum, but with some regard to presentational clarity. Thus, the relative intensities within the same DF trace will be reliable, but not necessarily when comparing between two traces.

5. Expanded views of the 2D-LIF and DF spectra for the 790–1190 cm^{-1} region exciting via the 797 cm^{-1} and 804 cm^{-1} eigenstates. The spectral intensities are represented by colours, with red being the most intense through to blue being the least; black represents the zero background. See text for discussion of the assignments. The relative intensities in the 2D-LIF spectrum are as recorded, while the DF spectra have been adjusted to be qualitatively in agreement with the 2D-LIF spectrum, but with some regard to presentational clarity. Thus, the relative intensities within the same DF trace will be reliable, but not necessarily when comparing between two traces.

6. Expanded views of the 2D-LIF and DF spectra for the 1190–1590 cm^{-1} region exciting via the 797 cm^{-1} and 804 cm^{-1} eigenstates. The spectral intensities are represented by colours, with red being the most intense through to blue being the least; black represents the zero background. See text for discussion of the assignments. The relative intensities in the 2D-LIF spectrum are as recorded, while the DF spectra have been adjusted to be qualitatively in agreement with the 2D-LIF spectrum, but with some regard to presentational clarity. Thus, the relative intensities within the same DF trace will be reliable, but not necessarily when comparing between two traces. For the $14_3 20_2 m_x$ level, we are unable to be definitive of the value of x, which is thought to be 1 or 2 – see text and Ref. 20.

7. Expanded views of the 2D-LIF and DF spectra for the 1590–1790 cm^{-1} region exciting via the 797 cm^{-1} and 804 cm^{-1} eigenstates. The spectral intensities are represented by colours, with red being the most intense through to blue being the least; black represents the zero background. See text for discussion of the assignments. The relative intensities in the 2D-LIF spectrum are as recorded, while the DF spectra have been adjusted to be qualitatively in agreement with the 2D-LIF spectrum, but with some regard to presentational clarity. Thus, the relative intensities within the same DF trace will be reliable, but not necessarily when comparing between two traces.

8. Expanded views of sections of the 2D-LIF spectra across the 790–825 cm^{-1} region demonstrating the activity when exciting via 797 cm^{-1}, 804 cm^{-1} and 818 cm^{-1}. The spectral intensities are represented by colours, with red being the most intense through to blue being the least; black represents the zero background. See text for discussion of the assignments.

9. DF spectra of 1600–1750 cm^{-1} regions via different intermediate levels. See text for discussion of the assignments. Each trace has been normalized to the most intense band; thus, the relative intensities within the same DF trace will be reliable, but to compare intensities between traces, refer to Figure 7.

Figure 1

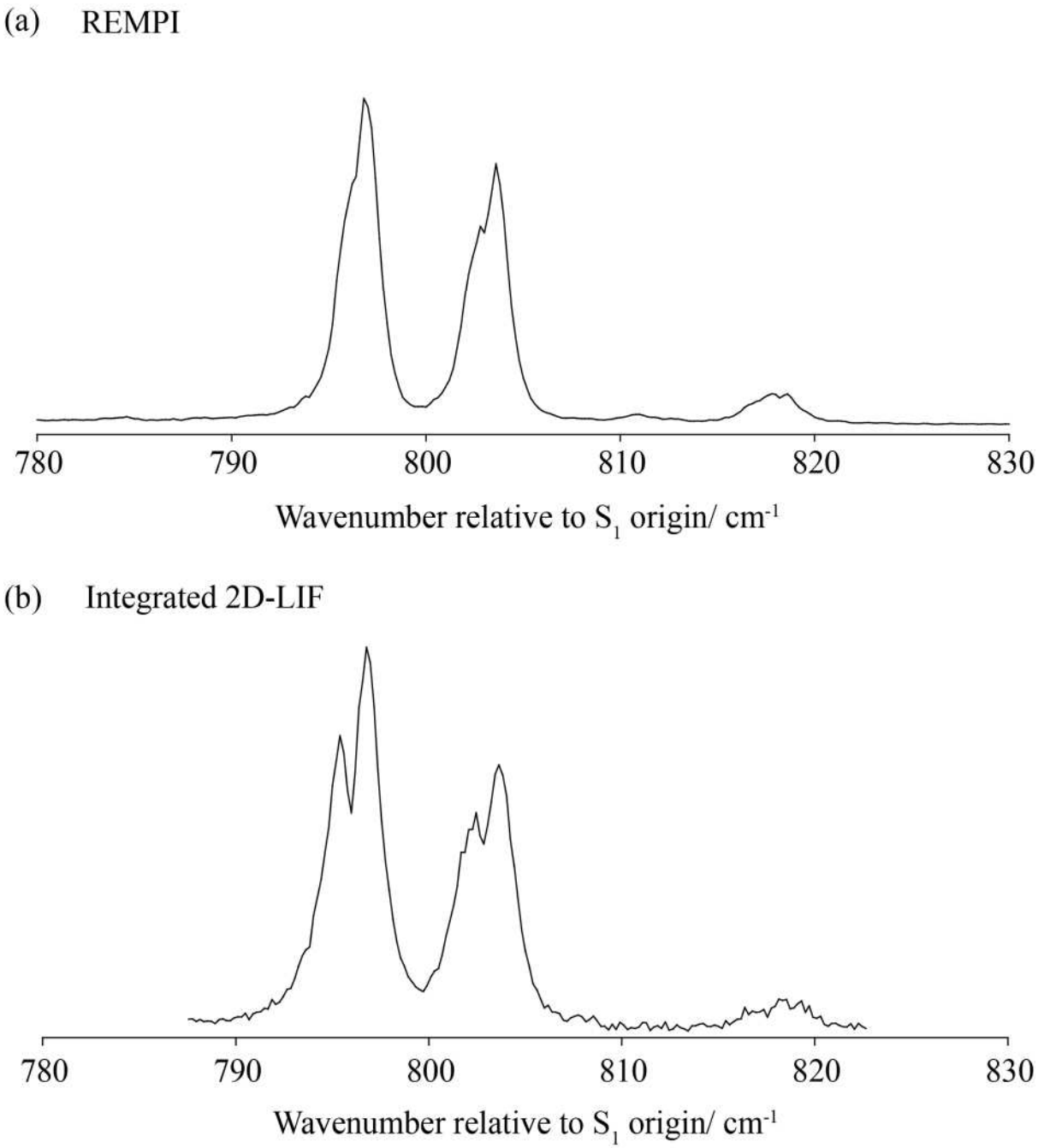
(a) REMPI
780
790
800
810
820
830
Wavenumber relative to S1 origin/ cm-1
(b) Integrated 2D-LIF
780
790
800
810
820
830
Wavenumber relative to S1 origin/ cm-1

Figure 2

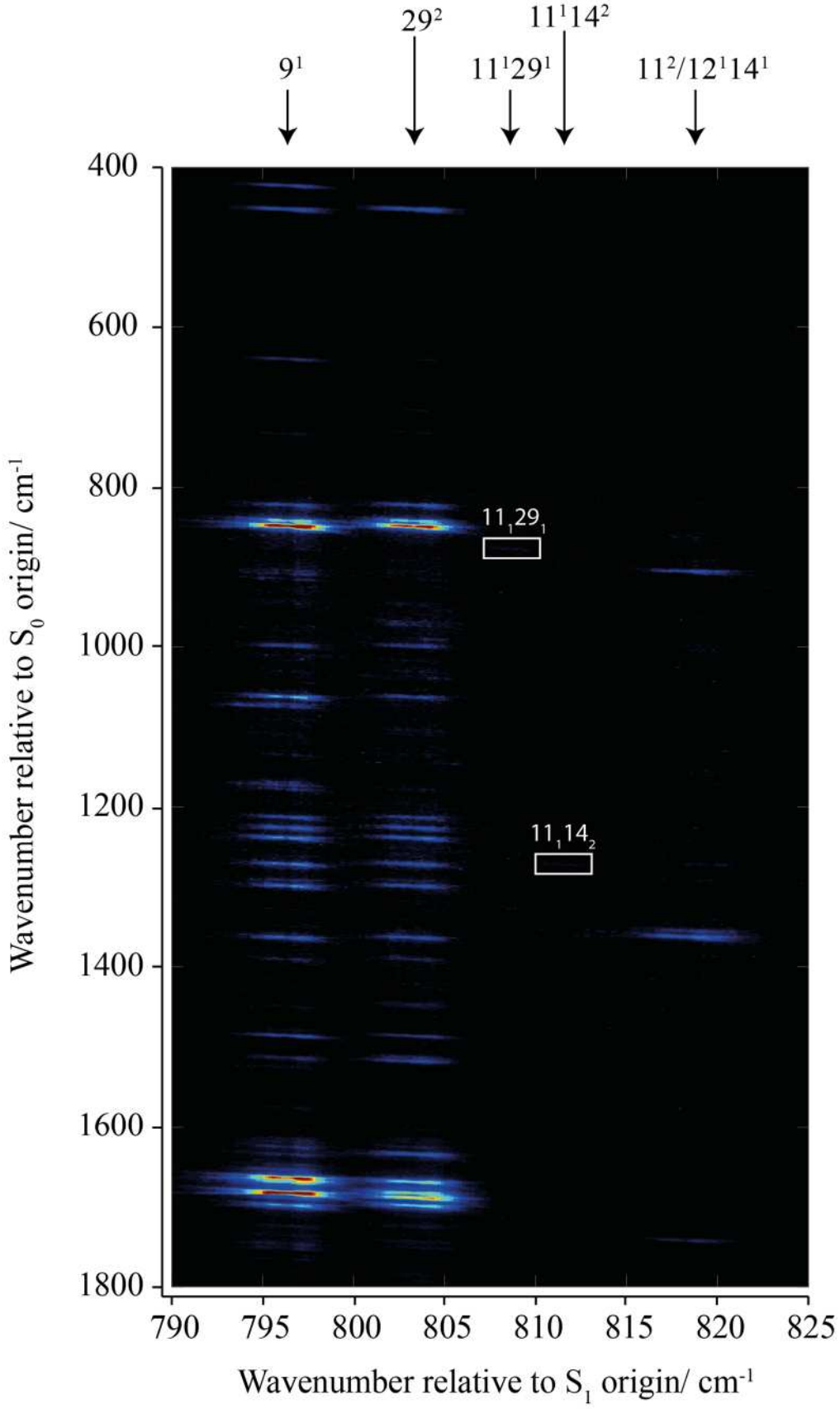
9^1
29^2
11^129^1
11^114^2
$11^2/12^114^1$
11_129_1
11_114_2
Wavenumber relative to S_0 origin/ cm^{-1}
400
600
800
1000
1200
1400
1600
1800
790
795
800
805
810
815
820
825
Wavenumber relative to S_1 origin/ cm^{-1}

Figure 3

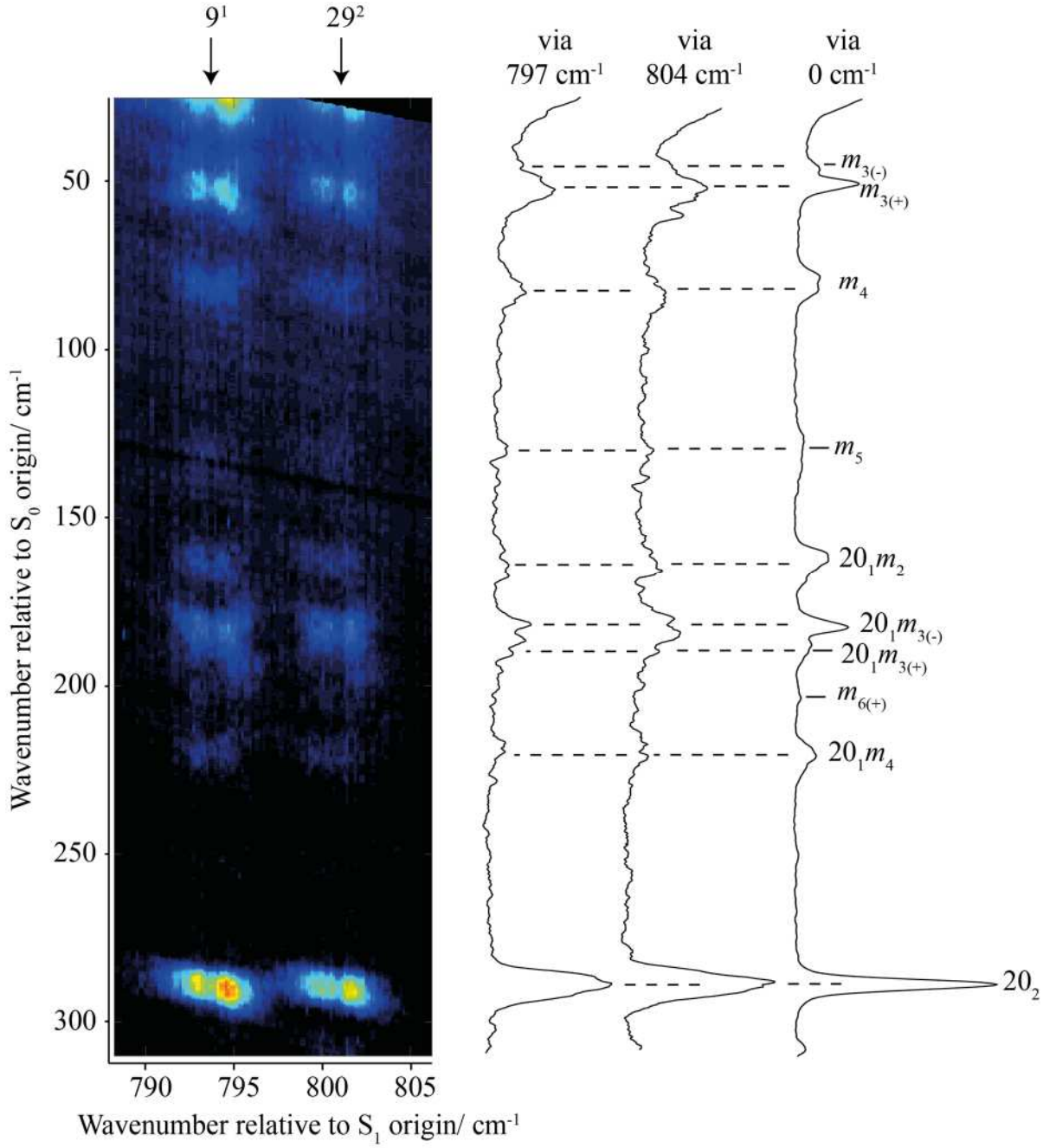
9¹
29²
via 797 cm⁻¹
via 804 cm⁻¹
via 0 cm⁻¹
m3(-)
m3(+)
m4
m5
20₁m2
20₁m3(-)
20₁m3(+)
m6(+)
20₁m4
20₂
Wavenumber relative to S0 origin/ cm⁻¹
50
100
150
200
250
300
790
795
800
805
Wavenumber relative to S1 origin/ cm⁻¹

Figure 4

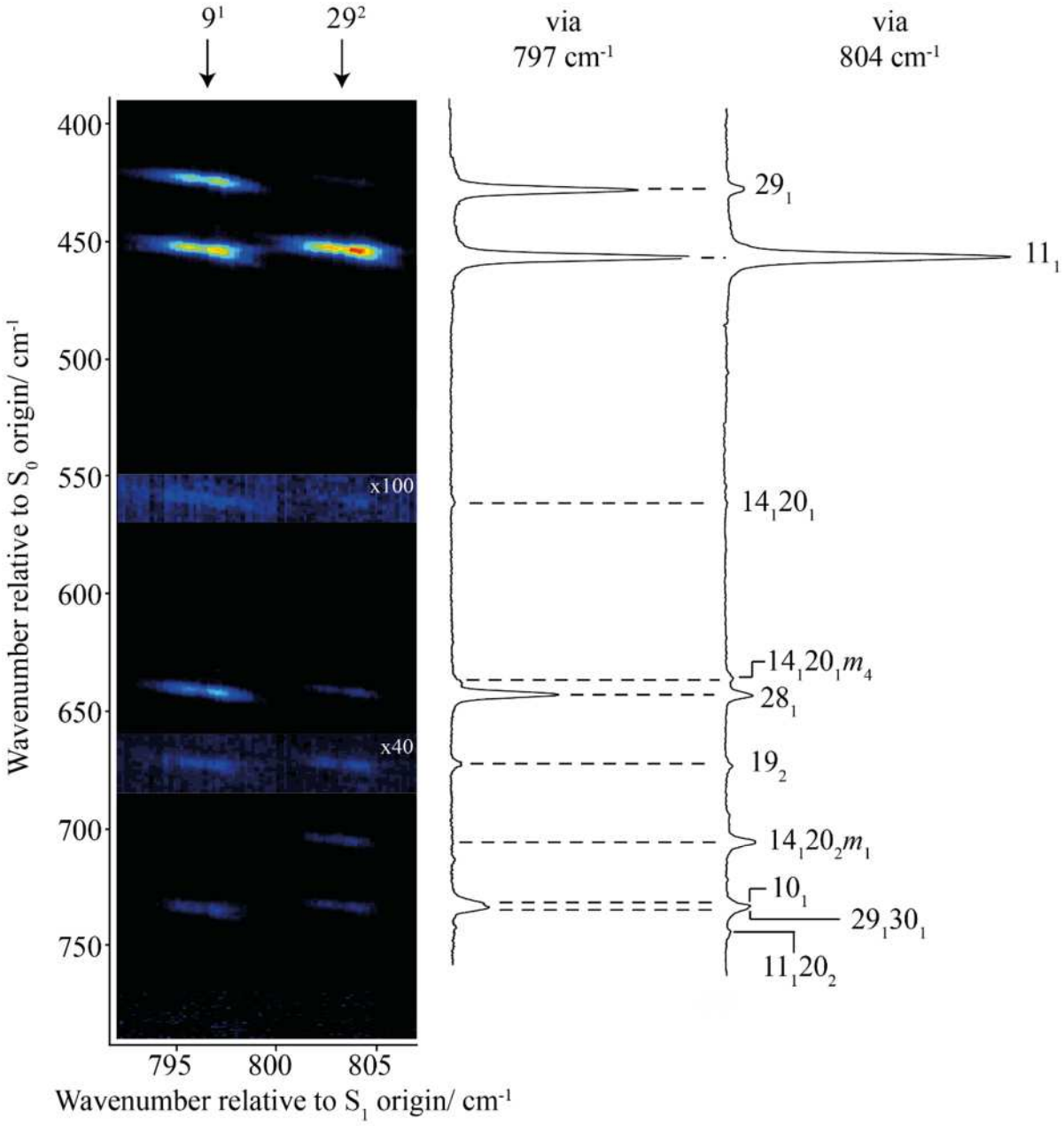
9¹
29²
via
797 cm-1
via
804 cm-1
400
450
500
550
600
650
700
750
x100
x40
Wavenumber relative to S0 origin/ cm-1
795
800
805
Wavenumber relative to S1 origin/ cm-1
29 1
11 1
14 1 20 1
14 1 20 1 m 4
28 1
19 2
14 1 20 2 m 1
10 1
29 1 30 1
11 1 20 2

Figure 5

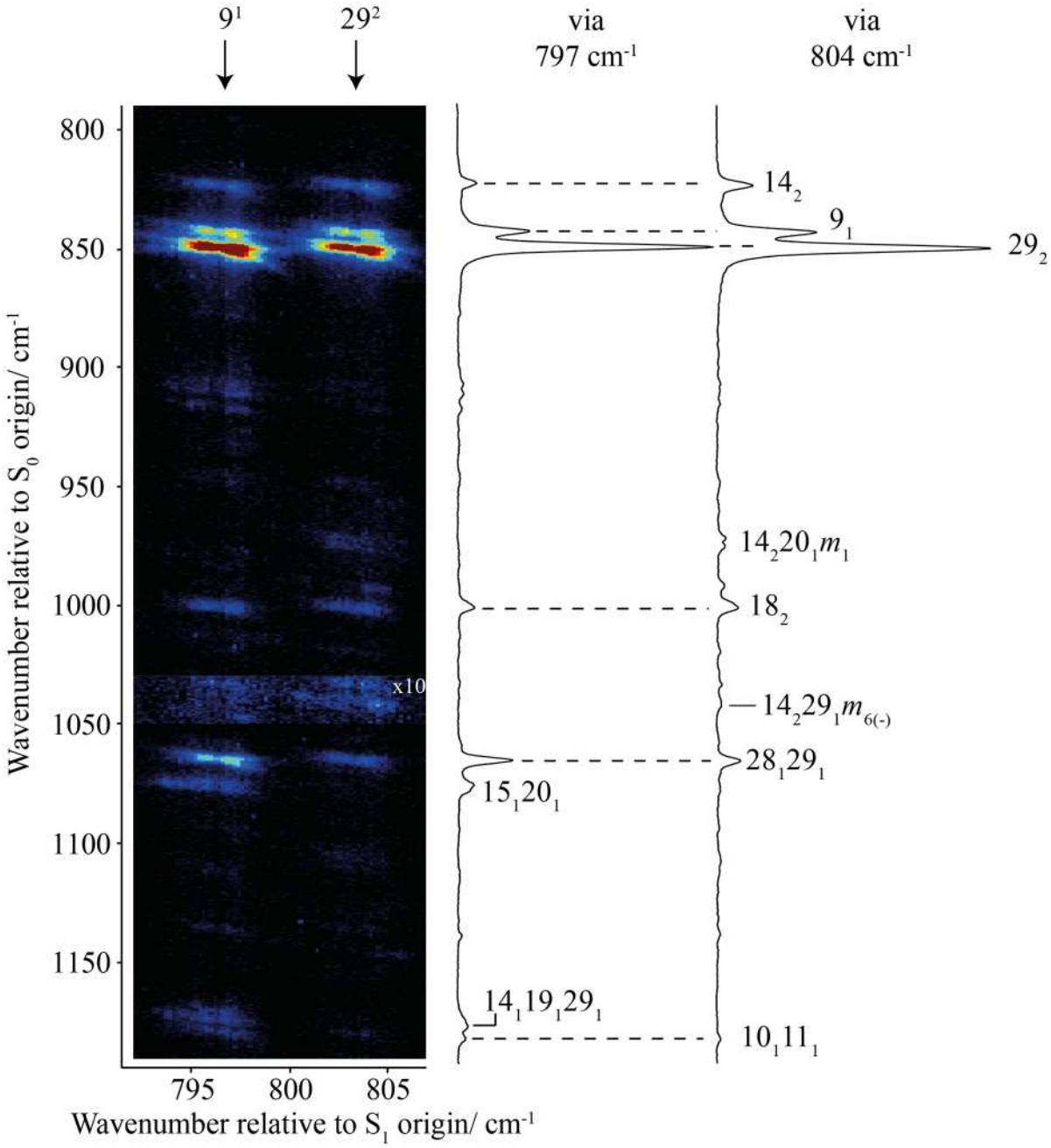
9¹
29²
via
797 cm-1
via
804 cm-1
800
850
900
950
1000
1050
1100
1150
x10
Wavenumber relative to S0 origin/ cm-1
795
800
805
Wavenumber relative to S1 origin/ cm-1
14 2
9 1
29 2
14 2 20 1 m 1
18 2
14 2 29 1 m 6(-)
28 1 29 1
15 1 20 1
14 1 19 1 29 1
10 1 11 1

Figure 6

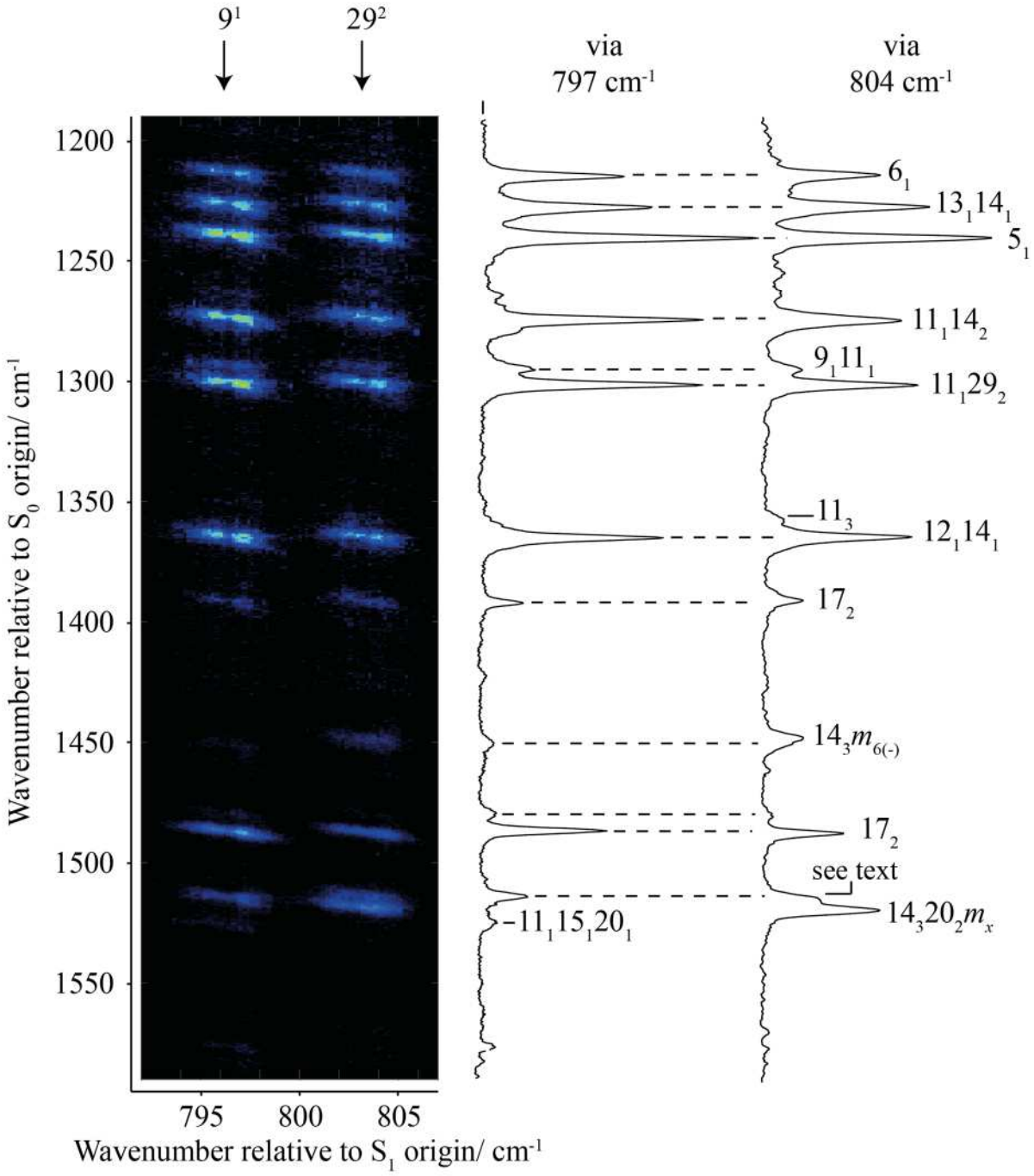
9¹
29²
via
797 cm⁻¹
via
804 cm⁻¹
1200
1250
1300
1350
1400
1450
1500
1550
Wavenumber relative to S0 origin/ cm⁻¹
795
800
805
Wavenumber relative to S1 origin/ cm⁻¹
6₁
13₁14₁
5₁
11₁14₂
9₁11₁
11₁29₂
11₃
12₁14₁
17₂
14₃m6(-)
17₂
see text
14₃20₂mx
11₁15₁20₁

Figure 7

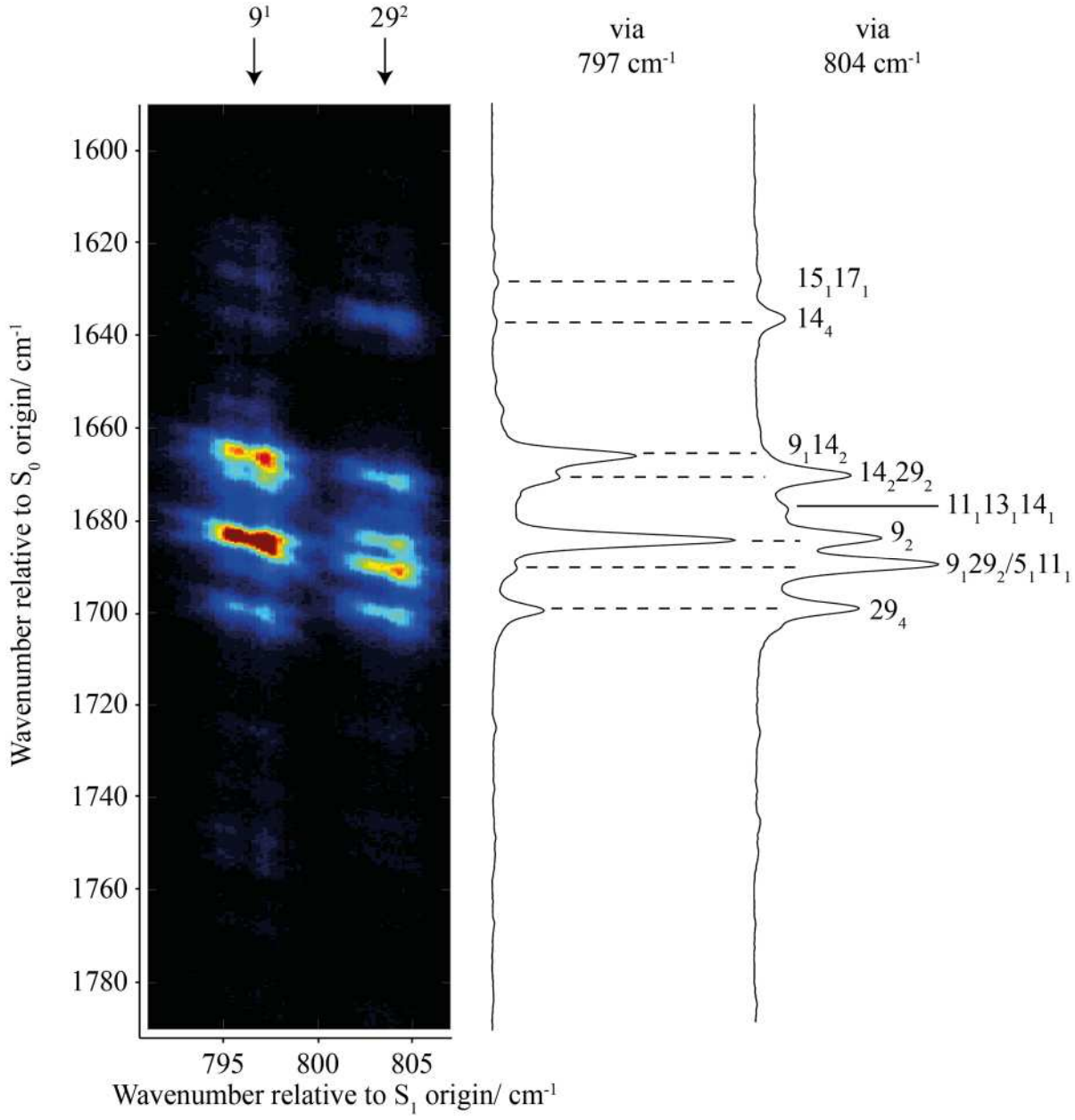
9¹
29²
via
797 cm-1
via
804 cm-1
15117
14⁴
9114²
14²29²
11113114
9²
9129²/5111
29⁴
1600
1620
1640
1660
1680
1700
1720
1740
1760
1780
Wavenumber relative to S0 origin/ cm-1
795
800
805
Wavenumber relative to S1 origin/ cm-1

Figure 8

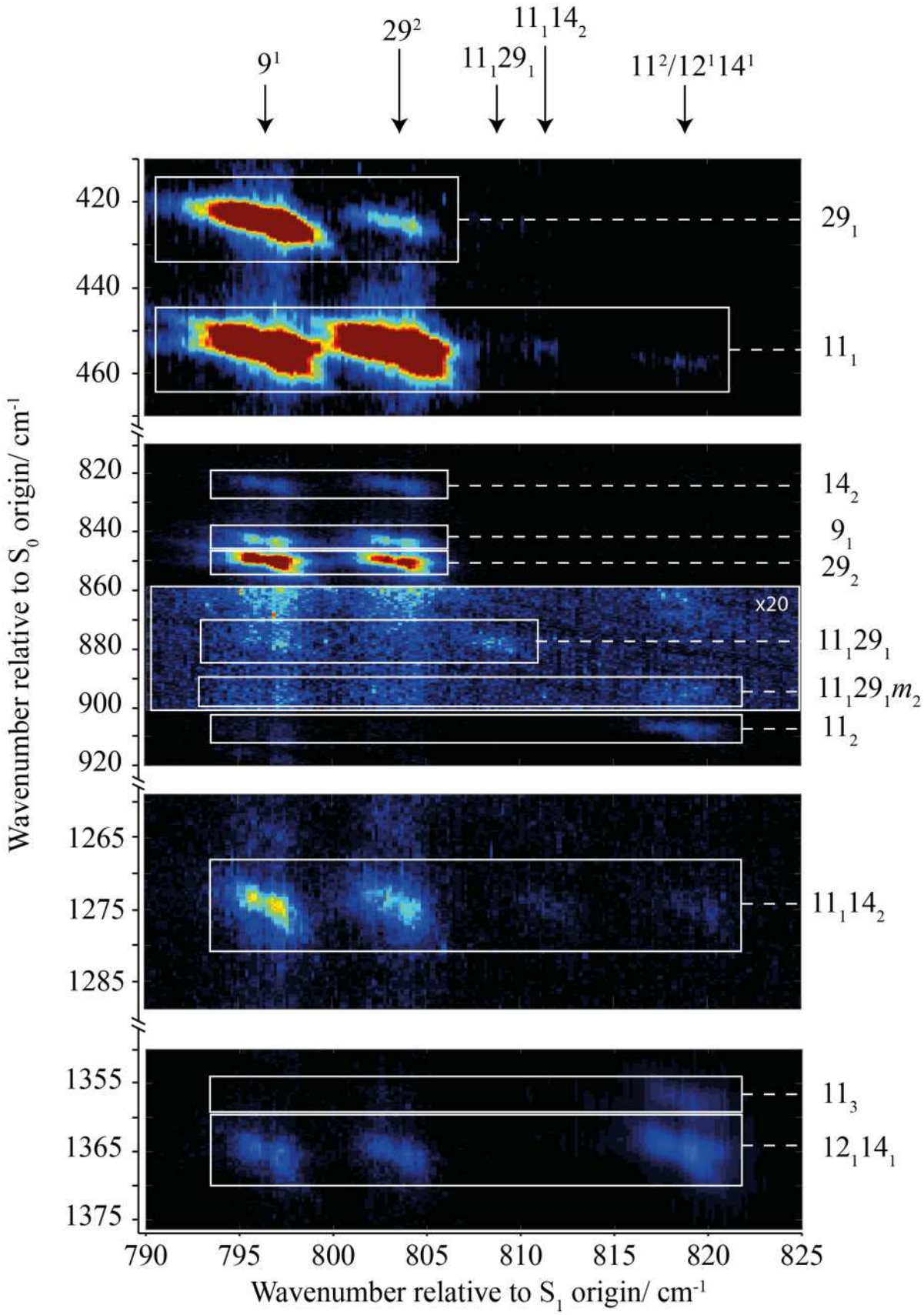
9¹
29²
11₁29₁
11₁14₂
11²/12¹14¹
29₁
11₁
14₂
9₁
29₂
x20
11₁29₁
11₁29₁m₂
11₂
11₁14₂
11₃
12₁14₁
Wavenumber relative to S₀ origin/ cm⁻¹
Wavenumber relative to S₁ origin/ cm⁻¹
420
440
460
820
840
860
880
900
920
1265
1275
1285
1355
1365
1375
790
795
800
805
810
815
820
825

Figure 9

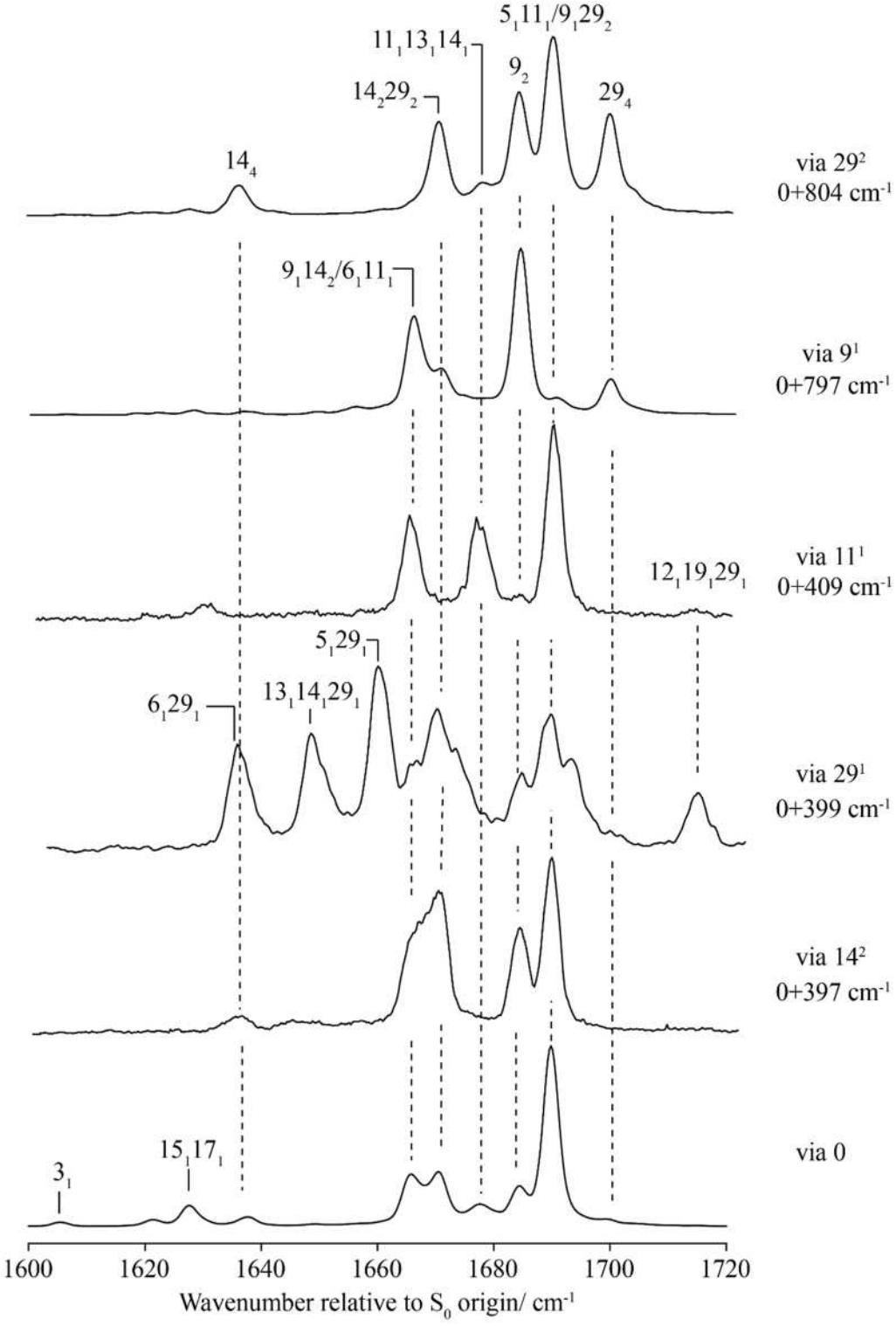
$5_1 11_1/9_1 29_2$
$11_1 13_1 14_1$
9_2
$14_2 29_2$
29_4
14_4
via 29^2
0+804 cm^{-1}
$9_1 14_2/6_1 11_1$
via 9^1
0+797 cm^{-1}
via 11^1
0+409 cm^{-1}
$12_1 19_1 29_1$
$5_1 29_1$
$6_1 29_1$
$13_1 14_1 29_1$
via 29^1
0+399 cm^{-1}
via 14^2
0+397 cm^{-1}
$15_1 17_1$
3_1
via 0
1600
1620
1640
1660
1680
1700
1720
Wavenumber relative to S_0 origin/ cm^{-1}

References

[1] Z.-Q. Zhao and C. S. Parmenter, *Mode Selective Chemistry* (Kluwer, 1991) Eds. J. Jortner, R. D. Levine, and B. Pullman. Jerusalem Symp. Quant. Chem. Biochem. **24**, 127 (1991).

[2] Z.-Q. Zhao, C. S. Parmenter, D. B. Moss, A. J. Bradley, A. E. W. Knight, and K. G. Owens, J. Chem. Phys. **96**, 6362 (1992).

[3] Z.-Q. Zhao, PhD Thesis, Indiana University (1992).

[4] Q. Ju, C. S. Parmenter, T. A. Stone, and Z.-Q. Zhao, Isr. J. Chem. **37**, 379 (1997).

[5] J. A. Davies, A. M. Green, A. M. Gardner, C. D. Withers, T. G. Wright, and K. L. Reid, Phys. Chem. Chem. Phys. **16**, 430 (2014).

[6] A. M. Gardner, A. M. Green, V. M. Tamé-Reyes, K. L. Reid, J. A. Davies, V. H. K. Parkes, and T. G. Wright, J. Chem. Phys. **140**, 114308 (2014).

[7] A. M. Gardner, A. M. Green, V. M. Tamé-Reyes, V. H. K. Wilton, and T. G. Wright, J. Chem. Phys. **138**, 134303 (2013).

[8] E. A. Virgo, J. R. Gascooke, and W. D. Lawrance, J. Chem. Phys. **140**, 154310 (2014).

[9] J. R. Gascooke, E. A. Virgo, and W. D. Lawrance, J. Chem. Phys. **142**, 024315 (2015).

[10] J. R. Gascooke, E. A. Virgo, and W. D. Lawrance, J. Chem. Phys. **143**, 044313 (2015).

[11] J. R. Gascooke and W. D. Lawrance, J. Molec. Spec. **318**, 53 (2015).

[12] W. D. Tuttle, A. M. Gardner, L. E. Whalley, and T. G. Wright, J. Chem. Phys. **146**, 244310 (2017).

[13] A. M. Gardner, W. D. Tuttle, L. E. Whalley, and T. G. Wright, Chem. Sci. **9**, 2270 (2018).

[14] V. L. Ayles, C. J. Hammond, D. E. Bergeron, O. J. Richards, and T. G. Wright, J. Chem. Phys. **126**, 244304 (2007).

[15] A. M. Gardner, W. D. Tuttle, L. Whalley, A. Claydon, J. H. Carter, and T. G. Wright, J. Chem. Phys. **145**, 124307 (2016).

[16] J. R. Gascooke, L. D. Stuart, P. G. Sibley, and W. D. Lawrance, J. Chem. Phys. **149**, 074301 (2018). This work contains considerable extra information in its supplementary information. Note, however, that the excitation wavenumber axis is incorrect in Figure S9.

[17] W. D. Tuttle, A. M. Gardner, L. E. Whalley, D. J. Kemp, and T. G. Wright, Phys. Chem. Chem. Phys. In Press. (2019) DOI: 10.1039/c8cp02757a

[18] A. M. Gardner, W. D. Tuttle, P. Groner, and T. G. Wright, J. Chem. Phys. **146**, 124308 (2017).

[19] W. D. Tuttle, A. M. Gardner, K. B. O'Regan, W. Malewicz, and T. G. Wright, J. Chem. Phys. **146**, 124309 (2017).

[20] "Unravelling overlaps and torsion-facilitated coupling using two-dimensional laser-induced fluorescence", D. J. Kemp, A. M. Gardner, W. D. Tuttle and T. G. Wright, Mol. Phys. (In press). https://doi.org/10.1080/00268976.2018.1554865

[21] J. R. Gascooke and W. D. Lawrance, Eur. Phys. J. D **71**, 287 (2017).

[22] W. T. Cave and H. W. Thompson, Faraday Soc. Trans. **9**, 35 (1950).

[23] T. Cvitaš and J. M. Hollas, Molec. Phys. **20**, 645 (1971).

[24] C. J. Seliskar, M. A. Leugers, M. Heaven, and J. L. Hardwick, J. Molec. Spectrosc. **106**, 330 (1984).

[25] K. Okuyama, N. Mikami, and M. Ito, J. Phys. Chem. **89**, 5617 (1985).

[26] Z.-Q. Zhao and C. S. Parmenter, Ber. Bunsenges. Phys. Chem. **99**, 536 (1995).

[27] J. A. Davies and K. L. Reid, Phys. Rev. Lett. **109**, 193004 (2012).

[28] E. B. Wilson, Jr, Phys. Rev. 45 (1934) 706.

[29] G. Varsányi, *Assignments of the Vibrational Spectra of Seven Hundred Benzene Derivatives* (Wiley, New York, 1974).

[30] R. S. Mulliken, J. Chem. Phys. **23**, 1997 (1955).

[31] G. Herzberg, Molecular Spectra and Molecular Structure II. Infrared and Raman Spectra of Polyatomic Molecules (Krieger, Malabar, 1991).

[32] A. M. Gardner and T. G. Wright, J. Chem. Phys. **135**, 114305 (2011).

[33] A. Andrejeva, A. M. Gardner, W. D. Tuttle, and T. G. Wright, J. Molec. Spectrosc. **321**, 28 (2016).

[34] P. J. Breen, J. A. Warren, E. R. Bernstein, and J. I. Seeman, J. Chem. Phys. **87**, 1917 (1987).

[35] E. Fermi, Z. Phys. **71**, 250 (1931).

[36] J. R. Gascooke and W. D. Lawrance, *J. Chem. Phys*., 2013, **138**, 134302.

[37] N. T. Whetton and W. D. Lawrance, *J. Phys. Chem.*, 1989, **93**, 5377–5384.

[38] A. E. W. Knight and S. H. Kable, J. Chem. Phys. **89**, 7139 (1988). Note that this work includes a significant number of further spectra and comments as part of the Supplementary Information.

[39] D. J. Kemp, A. M. Gardner, W. D. Tuttle, J. Midgley, K. L. Reid, and T. G. Wright, J. Chem. Phys. **149**, 094301 (2018).

[40] C. J. Hammond, V. L. Ayles, D. E. Bergeron, K. L. Reid, and T. G. Wright J. Chem. Phys. **125**, 124308 (2006).

[41] C. S. Parmenter and B. M. Stone, J. Chem. Phys. **84**, 4710 (1986).